Structure and Adsorption Properties of Activated Carbon Aerogels

Dingcai Wu, Zhuoqi Sun, Ruowen Fu

Materials Science Institute, Key Laboratory for Polymeric Composite and Functional Materials of Ministry of Education, Zhongshan University, Guangzhou, 510275, People's Republic of China

Received 5 January 2005; accepted 13 April 2005
DOI 10.1002/app.22764
Published online 9 December 2005 in Wiley InterScience (www.interscience.wiley.com).

ABSTRACT: Activated carbon aerogels (ACAs) with excellent microporosity (e.g., 0.44 cm^3/g) and mesoporosity (e.g., 1.72 cm^3/g) were prepared by CO_2 activation. Their structures were investigated with transmission electron microscopy and N_2 adsorption–desorption analysis. Subsequently, their adsorption properties toward organic vapors were studied with static and dynamic adsorption experiments. The micropores of the ACAs had stronger adsorption ability than those of normal porous carbons. Furthermore, the condensation of organic vapors in the mesopores of ACAs greatly enhanced their equilibrium adsorption at high relative pressures. As a result, the adsorption capacities of organic vapors on the typical ACAs prepared were about 2–3 times greater than those on normal porous carbons. In addition, they also possessed excellent adsorption dynamics and outstanding desorption and regeneration properties.
 J Appl Polym Sci 99: 2263–2267, 2006

Key words: adsorption; structure; synthesis

INTRODUCTION

Carbon aerogels (CAs) have been reported as promising materials that can be used as new absorbents.[1–3] Therefore, studies of the adsorption properties of CAs are of great significance both in science and in applications. Basically, CAs have abundant mesopores and a few micropores. Hanzawa et al.[4] successfully produced excellent microporosity to mesoporosity in CAs by activation, and this resulted in large surface areas comparable to those in activated carbon fibers (ACFs). Therefore, the activation would be especially helpful for the application of CAs as absorbents. However, to the best of our knowledge, thus far very little work has been reported on the porous structure and adsorption–desorption properties of activated carbon aerogels (ACAs). In this study, we prepared ACAs by CO_2 activation. The effects of the activation conditions on the structures of the ACAs thus obtained were investigated. Subsequently, the structure–adsorption property relationship of the obtained ACAs was studied with experiments on the adsorption of organic vapor. Their adsorption and desorption properties were compared with those of traditional porous carbons, such as activated carbons and ACFs.

Correspondence to: R. Fu (cesfrw@zsu.edu.cn).
Contract grant sponsor: National Nature Science Foundation of China; contract grant number: 50472029.
Contract grant sponsor: Foundation of Specialized Research Fund for the Doctoral Program of Higher Education.
Contract grant sponsor: Team Project and Scientific Foundation of Guangdong; contract grant numbers: 20003038 and 2004A30404001.

EXPERIMENTAL

Organic aerogels were synthesized by the sol–gel polymerization of resorcinol and formaldehyde, followed by ambient-pressure drying (24 h at room temperature, 12 h at 60°C, and 5 h at 110°C). Subsequently, the resultant organic aerogels were heated to 1173 K at a heating rate of 5 K/min and kept at this carbonization temperature for 3 h in an N_2 flow (800 mL/min). CAs thus obtained had a bulk density of 0.69 g/cm^3. After that, the CAs were ground into powder and heated at a heating rate of 5°C/min to a given activation temperature by a quartz tube furnace under an N_2 atmosphere, and then they were activated with 25 vol % CO_2 for a predetermined activation time. After the samples cooled down, ACAs were obtained, and they were labeled ACA-*xxx*-*yyy*, where *xxx* and *yyy* denote the activation temperature and activation time, respectively.

The nanoparticle structures of the ACAs and related CA were observed with a JEOL JEM-2010H transmission electron microscopy (TEM) instrument (Tokyo, Japan). The nitrogen adsorption and desorption isotherms of the samples were taken with an ASAP 2010 surface area analyzer (Micromeritics Instrument Corp. (Atlanta, GA)), and their Brunauer–Emmett–Teller

TABLE I
Pore Parameters of the ACAs

Sample	Burn-off (wt %)	S_{BET} (m^2/g)	S_{mic} (m^2/g)	S_{mes} (m^2/g)	V_{mic} (cm^3/g)	V_{mes} (cm^3/g)
CA	0	608	343	318	0.16	0.86
ACA-900-1h	31.4	974	590	440	0.28	1.08
ACA-900-2h	45.4	1165	718	517	0.33	1.24
ACA-900-3h	57.1	1399	857	577	0.40	1.36
ACA-750-2h	10.5	648	383	318	0.18	0.83
ACA-950-2h	78.2	1817	952	809	0.44	1.72
VACF[a]		909	787	58	0.39	0.04
SNACF		800–1000			0.35	
PACF		1300–1700				
GAC1[a]		451	374	48	0.18	0.04
GAC		900				

The adsorption data of SNACF, PACF, and GAC were from ref.[5]
[a] VACF and GAC1 were obtained from Liaoyuan Chemical Material Factory of China Chemical New Material Corp. (Liaoyuan City, China) and Zengcheng Liansheng Activated Carbon Factory (Zhengcheng City, China), respectively.

(BET) surface area (S_{BET}), micropore volume (V_{mic}), micropore surface area (S_{mic}), mesopore volume (V_{mes}), mesopore surface area (S_{mes}), and pore size distribution were analyzed correspondingly. The static adsorption measurements of the ACAs toward organic vapors were carried out at 30°C by a weight method. The desorption of the samples for different organic vapors was carried out by the exposure of the adsorbed samples to air at a predetermined temperature. The dynamic adsorption properties of the obtained ACAs were studied with an IG-3 intelligent gravimetric analyzer (Hiden Isochema, Ltd., Warrington, UK).

RESULTS AND DISCUSSION

Table I shows the pore parameters of the ACAs and the related CA thus obtained. S_{BET} and S_{mic} of the ACAs greatly increased after activation. Also, S_{mes} and V_{mes} increased to a certain extent after activation. S_{BET} of the ACAs could reach the same level as that of normal ACFs, such as viscose-fiber-based activated carbon fiber (VACF), sulfonic-group-containing polyacrylonitrile-based activated carbon fiber (SNACF), and pitch-based activated carbon fiber (PACF).[5] The experimental results indicated that S_{BET}, S_{mic}, and V_{mic} of the ACAs increased with increasing activation temperature and activation time. However, as for normal porous carbons, the burn-off of the ACAs obviously increased with increasing activation temperature and activation time. Therefore, in most cases, the limit on the upper activation temperature and activation time should depend on the balance of improvements in the porosity and activation yield.

Figure 1 presents TEM photographs of a representative ACA and its precursor CA. The ACA kept the same three-dimensional nanonetwork structure of the precursor CA, although the nanoparticle size of the ACA slightly decreased because of the burn-off during the activation process.

Figure 2 shows that the patterns of the pore size distributions of various ACAs and the related CA were the same, indicating that all of them possessed

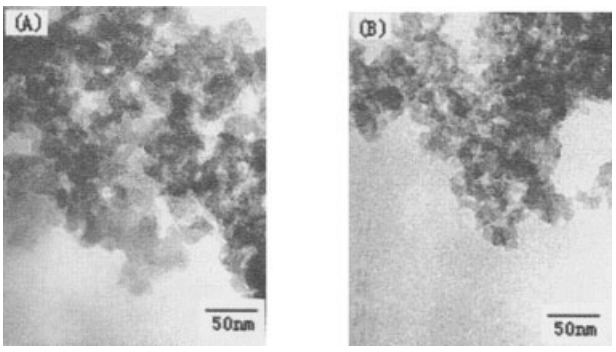

Figure 1 TEM photographs of CA and related ACA: (A) CA and (B) ACA-900-2h.

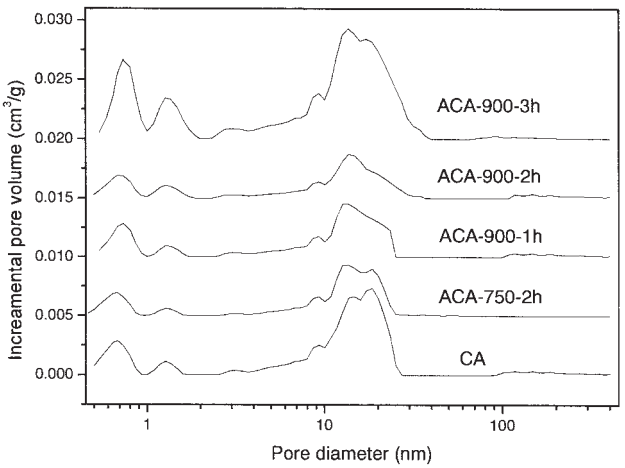

Figure 2 Pore size distributions of the ACAs.

TABLE II
Adsorption Capacities of Organic Vapors on the ACAs

Sample	Methanol		Acetone		Cyclohexane		Benzene	
	mg/g	mmol/g	mg/g	mmol/g	mg/g	mmol/g	mg/g	mmol/g
ACA-900-3h	1295	40.47	1218	21.00	1474	17.55	1513	19.40
ACA-950-2h	1605	50.16	1435	24.74	1584	18.86	1750	22.44
CA	590	18.44	737	12.71	764	9.10	806	10.33
SNACF	591	18.47	645	11.12	515	6.13	664	8.51
PACF	488	15.25	—	—	492	5.86	544	6.97
GAC	205	6.41	224	3.86	185	2.20	213	2.73

The adsorption data of SNACF, PACF, and GAC were from ref.[5]

the same pore geometry. That is, the micropores and mesopores of the ACAs that formed during activation were very similar to those of the CA that formed during carbonization. With increasing activation temperature and activation time, the numbers of micropores and mesopores of the ACAs increased, but the increasing tendency for the formation of micropores was noticeably larger than that of the mesopores.

Table II shows the adsorption capacities of various organic vapors on the ACAs and related CA. Surprisingly, the adsorption capacities of various organic vapors on the CA were much larger than that of granular activated carbon (GAC) and even slightly larger than those of SNACF and PACF.[5] Moreover, after activation, the adsorption capacities on the ACAs were about 2–3 times larger than those of SNACF and PACF, although their S_{BET} values were close. These results indicate that the porous structure of the ACAs thus prepared had a stronger adsorption ability than that of normal porous carbons, such as ACFs and GACs.

Figure 3 presents acetone-vapor adsorption–desorption isotherms of representative ACA, CA, ACF, and GAC samples. The isotherms of the ACA and CA are obviously different from those derived from the ACF and GAC. The former has a large hysteresis loop at a high relative pressure, illuminating the existence of numerous mesopores, whereas the latter has a quite small hysteresis loop at a high relative pressure, although all of the isotherms rise sharply at a low relative pressure, indicating the existence of numerous micropores. Figure 3 shows that in the range of low relative pressures, the ACA had a higher adsorption capacity for acetone than the VACF. For example, the adsorption capacities of acetone on the ACA-900-2h and on the VACF were 405 and 284 mg/g, respectively, at a relative pressure of $P/P_0 = 0.4$ (where P is adsorption pressure and P_0 is the situation vapor pressure at adsorption temperature), although their S_{mic} and V_{mic} values were at the same level (see Table I). This indicates that the micropores of the ACAs thus prepared had much higher adsorption efficiency than those of ACFs, most likely because of the nanosize of the carbon particles and the direct exposure of the micropores over the whole surface of the carbon nanoparticles. When the relative pressure was over 0.55, the adsorption capacity of acetone on the ACA in-

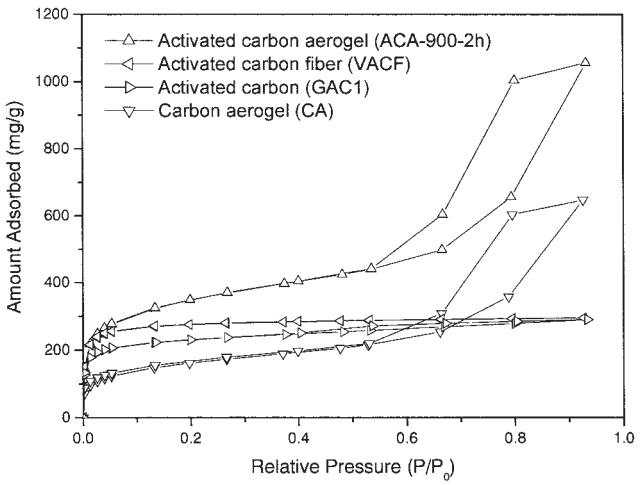

Figure 3 Adsorption–desorption isotherms of acetone vapor on porous carbon samples (30°C).

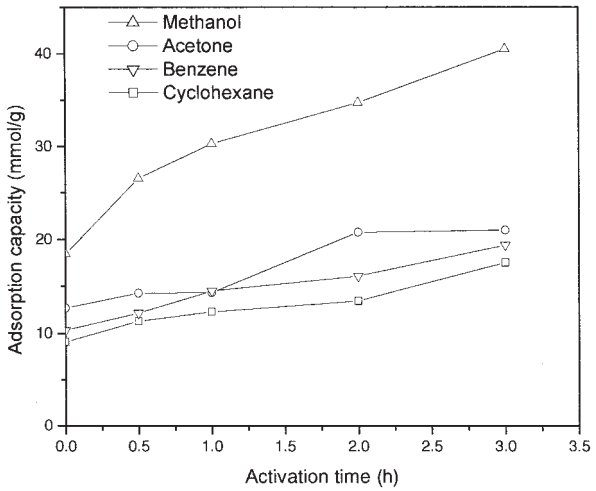

Figure 4 Influence of the activation time on the adsorption capacities of organic vapors on the ACAs.

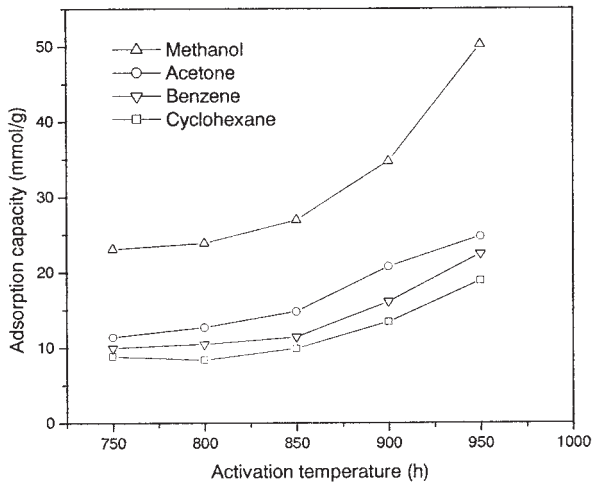

Figure 5 Influence of the activation temperature on the adsorption capacities of organic vapors on the ACAs.

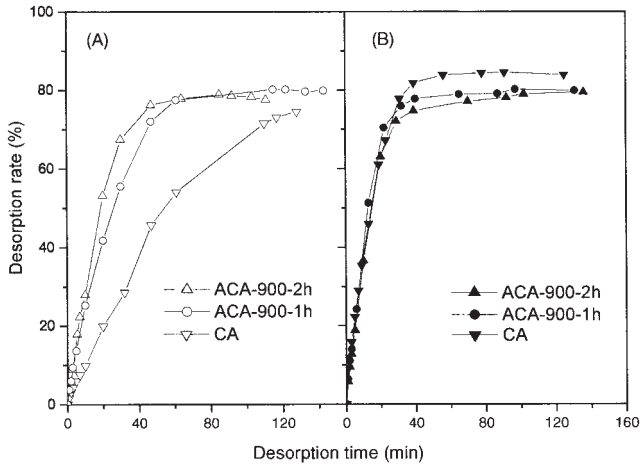

Figure 7 Desorption rate of the ACAs in air at room temperature: (A) methanol and (B) cyclohexane.

creased quickly and reached about 1056 mg/g at $P/P_0 = 0.93$ because of the condensation of acetone vapor in the mesopores of the ACA. Therefore, the strong vapor adsorption ability of the ACAs could be attributed to micropore filling at a low relative pressure and mesopore condensation at a high relative pressure. This deduction was also supported by the fact that the vapor adsorption capacities of the ACAs increased with increasing activation time or activation temperature, both of which caused an increase in micropores and mesopores (see Table I and Figures 4 and 5).

The experimental results for dynamic adsorption behavior in Figure 6 indicate that the adsorption speed of the ACAs for acetone was much higher than that of the CA and GAC1 and close to that of the VACF.

The large adsorption capacity and high adsorption speed of the ACAs for organic vapors could most likely be attributed to the large increase in the microporosity and also the better accessibility of these micropores formed during the activation because they were on easily accessed nanoparticles.

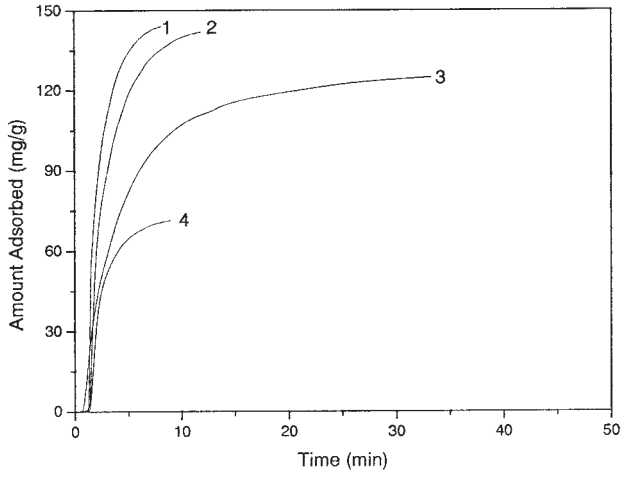

Figure 6 Adsorption speed of porous carbon samples for 1-mb acetone vapor: (1) VACF, (2) ACA-900-2h, (3) GAC1, and (4) CA.

In this study, the desorption and regeneration properties of the ACAs were also investigated, and the experimental results are shown in Figure 7 and Table III. Figure 7 shows that the desorption rates of the ACAs for various organic vapors reached about 80% even at room temperature; this outclassed the rates of various ACFs (20–35%).[6] Furthermore, the desorption and regeneration properties of ACAs at high temperatures (e.g., 110°C) were as good as those of ACFs reported.[5,6] The desorption rates of the ACAs could be increased to 95–100% by a heat treatment at 110°C. In addition, the regenerated ACAs had excellent renewable properties on the basis of their second adsorption capacity and regeneration efficiency in Table III.

CONCLUSIONS

ACAs activated by CO_2 possessed high S_{BET} values that reached the level of normal ACFs. All porous structure parameters of the ACAs, including S_{BET}, S_{mic}, V_{mic}, S_{mes}, and V_{mes}, increased with increases in the activation temperature and activation time, but all the ACAs possessed the same pore geometry as related CA. The porous structure of the ACAs had a stronger adsorption ability than that of normal porous carbons. The adsorption capacities of organic vapors on the prepared ACAs were about 2–3 times larger than those on SNACF and PACF. The adsorption speed of the ACAs for organic vapors was much higher than that of GACs and close to that of ACFs. Moreover, the obtained ACAs had outstanding desorption and regeneration properties.

TABLE III
Desorption and Regeneration Properties of the ACAs

	Methanol			Cyclohexane		
Sample	Desorption rate (%)	Second adsorption capacity (mg/g)	Regeneration efficiency (%)	Desorption rate (%)	Second adsorption capacity (mg/g)	Regeneration efficiency (%)
ACA-750-2h	99.2	734	99.4	99.2	725	97.7
ACA-800-2h	99.8	750	98.2	99.1	635	90.6
ACA-850-2h	100.5	860	99.8	95.9	816	98.2
ACA-900-2h	100.7	1144	103.0	94.7	1131	100.3
ACA-950-2h	100.0	1518	94.6	96.6	1604	101.3
ACA-900-0.5h	99.6	860	101.2	94.4	964	101.5
ACA-900-1h	99.9	907	93.6	94.5	1039	100.7
ACA-900-3h	100.1	1279	98.8	95.5	1393	94.5
CA	99.3	549	93.0	96.7	741	96.9

References

1. Bekyarova, E.; Kaneko, K. Adv Mater 2000, 12, 1625.
2. Fu, R.; Zheng, B.; Liu, J.; Dresselhaus, M. S.; Dresselhaus, G.; Satcher, J.; Baumann, T. Adv Funct Mater 2003, 13, 558.
3. Tamon, H.; Ishizaka, H.; Arak, T.; Okazaki, M. Carbon 1998, 36, 1257.
4. Hanzawa, Y.; Kaneko, K.; Pekala, R. W.; Dresselhaus, M. S. Langmuir 1996, 12, 6167.
5. Fu, R. W. In Functional Polymer Materials; Ma, J. B., Ed.; Chemical Industry: Beijing, 2000; p 80.
6. Fu, R.; Zhang, Y.; Fang, M.; Zeng, M. Chin J Mater Res 2000, 14, 367.